Multiple functionally and temporally independent selection mechanisms mediate working memory-guided behaviors

Edward F. Ester[1,2], Rachel Weese[1]

[1]Department of Psychology, University of Nevada, Reno
[2]Integrative Neuroscience Program, University of Nevada, Reno

Support: NSF 2050833 (E.F.E.), Nevada Undergraduate Research Award (R.W.)

Contributions: E.F.E. and R.W. conceived and designed the experiment. R.W. collected data, E.F.E. and R.W. analyzed data. E.F.E. and R.W. wrote the manuscript.

Data and Analytic Software: Stimulus presentation software, raw and preprocessed data, and analytic software are freely accessible via the Open Sciences Framework: https://osf.io/872tm/

Abstract

Recent theoretical conceptualizations of visual working memory (WM) have begun to emphasize the action-oriented nature of this system. To guide behavior, information stored in WM must be selected and mapped onto task-appropriate responses. Several physiological signals associated with the selection of task-relevant WM content have been identified, but it is unclear whether these signals index unique selection mechanisms. Here, we independently tracked and compared several electrophysiological and oculomotor signals previously linked with the selection of WM content. The data reveal a rich tapestry of functionally and temporally independent signals associated with the selection of visuospatial and visual feature information, as well as the selection of task-appropriate responses. Theoretical models of internal selective attention and WM-guided behavior will need to account for interactions between processes indexed by these signals.

A fundamental purpose of any memory system is to inform future decisions and actions. This is particularly important in the case of working memory (WM), a duration- and capacity-limited system that forms a temporal bridge between fleeting sensory phenomena and possible actions (1). Recent theoretical conceptualizations of WM have begun to emphasize the action-oriented nature of this system (e.g., 2-5), and recent empirical findings suggest that behavioral (6-7), circuit-level (8-10), and systems-level (11-20) mechanisms of WM storage and action planning are tightly interwoven.

Changing environmental circumstances and evolving behavioral goals necessitate the existence of internal selection mechanisms that prioritize task-relevant WM content for action, especially when an agent must select from among multiple prospective actions (e.g., 21-22). What is meant by “selection”, however, is ill-defined. Several conceptually (and physiologically) distinct signals have been used to track the selection of WM content following changes in behavioral priority (see 3 for a recent synopsis). To develop a coherent model of internal selection and WM-guided behavior, it is necessary to identify and integrate findings across these measurements. Here, we describe a study that facilitates this goal by simultaneously tracking – in near-real-time – and comparing several different physiological signals thought to index the selection of task-relevant WM contents and task-appropriate motor plans.

Human volunteers performed a WM task requiring them to recall one of two orientations stored in WM (Fig 1A). Before recall, a retrospective color cue instructed participants which orientation would be probed for report at the end of the trial and which hand should be used to respond (i.e., left vs. right). Following earlier work (17), we manipulated the physical location of the retrospectively cued orientation (i.e., left vs.

right visual field) independently of response hand; this allowed us to track electrophysiological correlates of covert spatial attention and motor preparation in trial-averaged EEG and oculomotor data. Unlike prior work, we decoupled attention shifts from response execution by delaying orientation recall until one second after the appearance of the retrocue, and we used multivariate pattern analysis to track the selection of orientation (i.e., the feature participants were required to report) independently of location (an incidental task feature). To preview the findings, electrophysiological signals associated with motor preparation began shortly after cue onset and persisted through the ensuing response period; electrophysiological and oculomotor signals associated with shifts of covert spatial attention emerged simultaneously with motor preparation but ended well before response onset. Critically, above-chance decoding of orientation was delayed until the onset of the response display, suggesting that the selection of task-relevant mnemonic information (orientation) is decoupled from the selection of task-irrelevant mnemonic information (location) and motor planning. Thus, the results point to the existence of multiple functionally and temporally independent internal selection mechanisms collectively responsible for the planning and execution of WM-guided behaviors.

Results

We recorded EEG from a custom scalp montage (Fig 1B) while 31 human volunteers performed a retrospectively cued orientation memory task (Fig 1A). The custom scalp montage strategically oversampled posterior occipitoparietal electrode sites where visual signals were assumed to be largest. Participants remembered the orientations of two gratings over a blank delay. 1.5 sec after encoding, a 100% valid color cue indicated which of the two gratings would be probed for report at the end of the trial and which hand should be used for memory recall (i.e., left or right; response hand/cue color mappings were counterbalanced across participants). A response display containing a vertically oriented grating was presented 1.0 seconds later; participants adjusted the orientation of this probe to match the orientation of the grating held in memory using the cued response hand. Participants performed this task well, recalling the orientation of the probed grating with an average (±1 S.E.M.) absolute error of 13.6° ± 0.75° and responded with the correct hand on 93.8% ± 0.89% of trials. The average response time (i.e., elapsed time between the onset of the probe display and the participant's initial button press) was 451 ±14.9 msec.

Parallel Selection of Spatial and Motor Information in WM

Following earlier work (17), we first identified EEG signals that co-varied with the physical location of the retrospectively cued stimulus (i.e., left vs. right visual hemifield) and EEG signals that co-varied with the retrospectively cued response hand (i.e., left vs.

Figure 1. Task Schematic and Recording Montage. (A) Schematic depicting a representative experimental trial. Displays are expository and not drawn to scale; see main text and methods for a complete task description and display/stimulus geometry. (B) Custom EEG recording montage.

right). Because stimulus location and response hand were independently manipulated over trials (i.e., a stimulus requiring a right-hand response was equally likely to appear in the left vs. right visual field) we were able to characterize the selection of both attributes in trial-averaged EEG data independently of one another and any nuisance effects (e.g., volume conduction or other signal mixing). We therefore attributed patterns of neural activity that covaried with stimulus location to the selection of visual information stored in WM and patterns of neural activity that covaried with response hand to the selection of motor information stored in WM. While this approach is familiar from earlier work (e.g., 17), our task additionally allowed us to probe the dynamics of visuomotor selection during development of a *planned* action: upon presentation of retrocue display participants were free to select task-relevant visuomotor representations stored in WM but could not execute a response until one second later.

Visual selection was associated with a robust but transient decrease in 8-13 Hz alpha power over electrode sites contralateral to the location of the cued stimulus (Fig 2A). This modulation was strongest over occipitoparietal electrode sites (Fig 2B),

Figure 2. Spectral and Oculomotor Signals of Internal Selection. (A) Spectral signals that co-varied with stimulus location (i.e., left vs. right visual field). Vertical lines at time 0.0 and 1.0 depict the onset of the retrocue and probe displays, respectively. (B) Scalp distribution of alpha-band (8-13 Hz) activity shown in Panel A. (C) Spectral signals that co-varied with response hand (i.e., left vs. right), and (D) scalp distribution of mu-alpha (8-13 Hz) and beta (15-30 Hz) activity shown in Panel C. Conventions are identical to Panels A, B. (E) Time courses of lateralized occipitoparietal alpha, frontocentral mu-alpha, and frontocentral beta power. Horizontal bars mark periods where lateralization was significantly greater than 0, or where lateralization in one frequency band exceeded lateralization in a different frequency band (two-tailed, cluster-corrected randomization tests; see Methods). (E) Gaze bias, expressed as a percentage along the horizontal meridian towards the location of the retrospectively cued stimulus. A bias of 0.0% represents perfect fixation; a bias of -100% represents foveation of the cued stimulus (biases were sign-reversed to facilitate comparisons with the EEG data shown in Panel E). The horizontal blue bar at the top of the plot indexes periods where gaze bias was significantly < 0%. Shaded areas in Panels E and F depict the 95% confidence interval of the mean; vertical lines at times 0.0 and 1.0 depict the onset of the retrocue and probe displays, respectively.

consistent with prior reports linking changes in lateralized alpha power to shifts of attention in perception and WM (17; 23-24). Conversely, motor selection was associated with a robust and sustained decrease in 8-13 Hz mu-alpha power and 15-30 Hz beta power over electrode sites contralateral to the location of the cued response hand (Fig 2C). This modulation was strongest over frontocentral electrode sites (Fig 2D; inset), consistent with prior reports linking changes in lateralized mu-alpha and beta power to response preparation and execution (25). Direct comparisons of EEG signals associated with visual and motor selection revealed transient visual selection lasting approximately 250-850 ms and sustained motor selection lasting 250-3000+ ms after retrocue onset. These observations are difficult to reconcile with models of WM-guided behavior that require the continuous selection of visual information (e.g., 17) but can be explained by a hybrid selection model where visual WM representations are selected and transformed from a stimulus-specific to a response-specific format (e.g., 26-27).

Oculomotor Signatures of Spatial Selection

A handful of recent studies have reported small but robust biases in gaze (28-30) and head direction (31) towards the physical location of a retrospectively cued stimulus held in WM, even in tasks where storage of spatial information is unnecessary. It has been suggested that these biases occur independently of physiological signals associated with covert spatial attention, but the evidence is mixed. For example, a recent study reported larger modulations of lateralized alpha-band activity during trials containing significant gaze biases compared to trials without gaze biases, but significant

lateralized alpha modulations were also observed in the absence of gaze biases (32). Similar findings were recently reported in nonhuman primate superior colliculus (33).

Motivated by these findings, we sought to compare the amplitudes and latencies of EEG and oculomotor signals of covert spatial attention. We obtained high-quality gaze recordings for 18 of the 31 participants who completed this study (EEG and gaze position data were acquired concurrently, see Methods). Following earlier work (28), we converted participants' horizontal eye position measurements into a normalized metric where 0% represents perfect fixation and 100% represents foveating the center of the cued stimulus. We observed a small (~4%) but robust bias in horizontal gaze position towards the cued stimulus beginning 282 ms after cue onset (Fig 2F). This latency was statistically indistinguishable from the onset of significant alpha and beta-band lateralization in the same participants (140 ms and 358 ms, respectively; $p = 0.306$ and 0.145, bootstrap tests; see Methods). However, gaze biases persisted for a significantly longer period than alpha band lateralization, with the former terminating 1186 ms after cue onset and the latter terminating 776 ms after cue onset (a difference of 410 ms; $p = 0.006$; bootstrap test). We note that these findings must be interpreted with caution, as the gaze biases and EEG data summarized in Fig 2 are fundamentally different physiological signals that were subjected to different preprocessing routines. Nevertheless, differences in the durations of gaze biases and EEG markers of covert selective attention selection support the view that these signals constitute partially independent measures of selection (32-33).

Temporally Dissociable Selection of Task-Relevant and Incidental Visual Information

Several lines of evidence indicate that the brain automatically retains spatial information in WM. Location-specific representations can be reconstructed from scalp EEG activity during WM tasks where location is irrelevant (34) and decoded from population spiking activity in prefrontal, parietal, and visual cortex following a cue that renders location irrelevant (e.g., 10). As noted above, human gaze (e.g., 28) and head position (31) are biased towards the location of a behaviorally prioritized item stored in WM, again in tasks where location is irrelevant. Conversely, changes in gaze position or shifts of covert spatial attention during WM can disrupt or introduce systematic biases in memory for visual features (e.g., color; 35-36), and memory guided comparisons for successively presented visual stimuli are impaired when they are rendered in different spatial positions (37-39). Indeed, automatic storage of visuospatial information in WM may enable the segregation of mental representations in retinotopic or spatiotopic coordinate frames and provide a common representational format for the encoding, storage, selection, and retrieval of task-relevant WM content (e.g., 40).

These points aside, we note that our memory task – like earlier work (e.g., 17) – required participants to report orientation, not location. Indeed, participants could “solve” the memory task by remembering two color-orientation bindings independently of where these bindings were physically rendered. One might be tempted to predict that that the time course of selecting orientation information stored in WM tracks covert shifts of attention towards physical location of the to-be-reported item, but we see no reason why this must be so. Thus, we used multi-electrode pattern analysis to obtain temporally resolved estimates of decoding accuracy for the cue-matching and cue-nonmatching orientations held in memory, reasoning that selection mechanisms should amplify

neural signals associated with the selected orientation, making it easier to decode (or equivalently, improving decoding performance relative to a pre-selection period; 41-46). Specifically, we computed trial-wise orientation decoding performance for the cued and uncued memory items using broadband EEG signals measured over occipitoparietal electrode site pairs O1/2, PO3/4, and PO7/8 and frontocentral electrode site pairs C1/2 and C3/4 (Figure 3). These analyses revealed robust decoding of the cued but not uncued stimulus orientations, but only during the response display. Two aspects of these results bear additional consideration. First, although above-chance orientation decoding was limited to the response period where a physically oriented stimulus was present on the screen, the onset of above-chance decoding performance over occipitoparietal electrode sites occurred significantly earlier (142 ms) than participants' average response times (i.e., the time which elapsed between presentation of the probe display and participants' first button press; M = 451 ms; p = 0.019, bootstrap test). Thus, it is unlikely that above-chance orientation decoding performance during the response display is a purely stimulus-driven artifact. Conversely, the onset of above-chance decoding performance over frontocentral electrode sites (392 ms) was statistically indistinguishable from participants' response times (p = 0.167), but was significantly

Figure 3. Orientation Decoding Performance. An orientation decoding metric was computed by quantifying the multivariate distance between orientation-specific activation patterns measured in independent training and test data sets (see Methods). (A) Decoding performance for the cue-matching and -nonmatching orientations computed from occipitoparietal electrode site pairs O1/2, PO3/4, and PO7/8. Decoding time series have been smoothed with a 50 ms Gaussian kernel. Vertical bars at times 0.0 and 1.0 depict the onset of the retrocue and probe displays, respectively; the horizontal bar at the top of the plot depicts intervals where cue-matching decoding performance was significantly greater than chance (i.e., 0), or when cue-matching decoding performance was significantly greater than cue-nonmatching decoding performance. Shaded areas depict the 95% confidence interval of the mean. (B) Decoding performance for the cue-matching and -nonmatching orientations computed from occipitoparietal electrode site pairs C1/2 and C3/4. Conventions are identical to Panel A.

later than the onset of above-chance decoding performance over occipitoparietal electrode sites ($p = 0.040$), consistent with a serial “hand-off” of information from occipitoparietal areas thought to encode stimulus-specific representations of memoranda (47-51) to frontocentral motor areas known to control manual responses (17).

Discussion

Flexible behaviors require dynamic sensory inputs to be compared with internal representations of beliefs and goals. Many of these comparisons are mediate by working memory (WM), which stores representations of sensory phenomena and possible actions (3, 17). There is growing appreciation that WM encodes representations of multiple prospectively relevant stimuli and responses to maximize behavioral flexibility (3). Thus, mechanisms are needed to select WM content that is most relevant for immediate behaviors. What is meant by “selection”, however, is ill-defined. As summarized elsewhere (3, 52-53), several conceptually (and physiologically) distinct signals have been used to track the selection of WM content following changes in behavioral priority, including gaze position (e.g., 28), head position (e.g., 31), scalp EEG (17, 44), fMRI (43), and multi-unit activity (10). Thus, the mechanisms responsible for guiding the selection of WM content are poorly understood, and future research must focus on identifying mechanisms indexed by different physiological measurements and integrating these findings into a coherent model. The work described in this paper represents a first step toward this goal: we deliberately designed our experimental task to be amenable to the study of multiple (putative) selection mechanisms, including those associated with the processing of stimulus location (a feature thought to provide a common coordinate frame or “scaffolding” for cognitive operations at multiple stages of processing; 40), processing of stimulus orientation (i.e., the task-relevant feature participants were required to report), and the selection/execution of task-appropriate motor responses. Moreover, a major advantage of our approach is that it utilizes measures with the temporal resolution necessary to

distinguish different components of human information processing (on the order of tens of milliseconds).

Our findings reveal a rich tapestry of functionally and temporally independent selection mechanisms: oculomotor and EEG signals associated with the selection of stimulus location began simultaneously, though the former lasted for significantly longer than the latter. Signals associated with motor selection began coincident with spatial selection (replicating earlier findings) but lasted for a significantly longer period (Fig 2A-E). Finally, orientation selection – i.e., the critical task-relevant feature which participants were required to report – began much later than either spatial or motor selection (Fig 3), as though participants had begun to prepare a motor response before accessing the information on which that response would be based. We emphasize that some caution is required when comparing temporal profiles of spatial, orientation, and motor selection. After all, we defined spectral signals associated with spatial and motor selection by isolating and extracting responses in specific sub-bands of the EEG signal (i.e., 8-13 Hz “alpha” and 15-30 Hz “beta”) activity, while analyses of gaze bias and orientation decoding were based on raw records of eye position and the broadband EEG signal, respectively. Nevertheless, many of the temporal differences reported here are on the order of several hundred milliseconds, or approximately an order of magnitude larger than temporal distortions caused by standard EEG filters (54).

To summarize, the findings reported here reveal the existence of multiple functionally, temporally, and physiologically distinct mechanisms that index different aspects of internal selective attention. A complete description of WM-guided behavior will require these mechanisms to be integrated into a working physiological model.

Methods

Research Participants. 32 human volunteers (both sexes) from the University of Nevada, Reno community completed a single 2.5-hour testing session in exchange for monetary remuneration ($15/h). All experimental procedures were approved by the local institutional review board. All volunteers self-reported normal or corrected-to-normal visual acuity and gave both written and oral informed consent before enrolling in the study. Data from one participant who completed the study were excluded from final analyses due to chance-level task performance (i.e., the participant used the correct response hand on only 52% of trials); thus, the findings reported here reflect the remaining 31 participants.

Testing Environment. Participants were seated in a dimly lit room for the duration of testing. Visual displays were generated in MATLAB and rendered on a 27-inch LCD monitor (1920 x 1080 resolution) cycling at 240 Hz using Psychophysics Toolbox software extensions (55). Participants were seated approximately 80 cm from the display (head position was not constrained). Participants responded via buttons on a standard US computer keyboard.

Visuomotor Recall Task. A task schematic is shown in Fig 1A. Each trial began with a 500 ms sample display containing two colored gratings (radius 4.5 degrees visual angle [DVA] from a viewing distance of 80 cm; 1.0 cycles/DVA) presented 7.0 DVA to the left and right of a central fixation point. The orientation of each grating on each trial was randomly and independently sampled (with replacement) from the set [20, 40, 60, 80, 120, 140, 160°), and a small amount of angular jitter (±1-5°) was added to each orientation on each trial to discourage verbal coding. Stimulus orientations were

counterbalanced across the entire experiment (though not necessarily within a single block of trials).

The sample display was followed by a 1500 ms blank display and a 1000 ms retrocue display where the fixation cross changed colors from black to either blue or red. The color of the retrospective cue instructed participants which grating would be probed at the end of the trial (i.e., blue or red) and which hand should be used to make a behavioral response (left or right). Cue color-response mappings (i.e., red cue/left hand vs. red cue/right hand) were counterbalanced across participants. Each trial ended with a 2000 ms probe display containing a vertically oriented grating; participants recalled the orientation of the cued grating by adjusting the probe grating to match the corresponding sample grating using the cue-specific response hand. If participants were satisfied with their response before the end of the 2000 ms, they were instructed to refrain from pressing any other buttons. Participants completed 3 (N = 1), 7 (N = 2), or 8 (N = 28) blocks of 72 trials.

EEG Acquisition & Preprocessing. Continuous EEG was recorded from 63 scalp electrodes using a BrainProducts actiCHamp system. We used a custom recording montage (Fig 1B) that strategically oversampled the posterior scalp to maximize orientation decoding performance. Online recordings were references to the left mastoid (10-20 site TP9) and digitized at 1 kHz. Offline, data were re-referenced to the algebraic mean of the left and right mastoids (using 10-20 site TP10 as the right mastoid reference). The following preprocessing steps were applied, in order: (1) resampling from 1 kHz to 500 Hz; (2) bandpass filtering from 1 to 50 Hz (zero-phase forward- and reverse- finite impulse response filters as implemented by EEGLAB software

extensions; 56); (3) identification, removal, and reconstruction of noisy epochs via artifact subspace reconstruction (implemented via EEGLAB; 57-58), (4) epoching from -1.0 to +5.0 sec relative to the start of each trial, and (5) application of a surface Laplacian to remove low spatial frequency components from the signal (59).

Eyetracking Data Acquisition and Preprocessing. We obtained high-quality binocular eye position data for 18 of 32 participants enrolled in the study. Eye position data were acquired using an SR Research Eyelink 1000 Plus infrared eyetracker operating in remote (i.e., “head-free”) mode and digitized at 500 Hz. The eyetracker was calibrated 2-3 times per testing session using a standard nine-point grid included with the tracker hardware. Eye positoin data were filtered for blinks and horizontal eye movements > 2 DVA, then epoched from -1000 to +5000 ms relative to retrocue onset. No other preprocessing steps were applied.

Spectral EEG Analyses. Spectral analyses focused occipitoparietal and frontocentral 10-20 electrode site pairs O1/2, PO3/4, PO7/8, C1/C2, and C3/C4; analyses were restricted to a period spanning -500 to +2500 after retrocue onset. We extracted broadband spectral power from each electrode on each trial using a short-time Fourier transform (STFT) with a frequency range from 1-40 Hz (in 0.25 Hz steps) using a 200 ms sliding window and 2 ms step size. Power was computed by squaring the absolute value of the complex Fourier coefficients within each STFT window. To quantify changes in lateralized activity during visual selection, we sorted power estimates at each occipitoparietal electrode site by the location of the retrospectively cued stimulus, i.e., contralateral vs. ipsilateral hemifield, and expressed this difference as a normalized percentage:

$$L_i = 100 \times \frac{(c_i - s_i)}{(c_i + s_i)}$$

where c_i and s_i are the trial-averaged responses of electrode *i* when the retrospectively cued grating appeared in the contralateral or ipsilateral visual field, respectively. Lateralization estimates were pooled across occipitoparietal electrode sites, yielding a single time-frequency matrix of power estimates per participant. An identical approach was used to quantify changes in lateralized activity during motor selection, with the exceptions that (a) analyses focused exclusively frontocentral electrode sites, and (b) trial-wise power estimates were sorted by the retrospectively cued response hand rather than stimulus location.

To generate topographical maps of alpha- and beta-band lateralization, we repeated this analysis for every scalp electrode and averaged power estimates over 8-13 Hz ("alpha-band" activity) and 15-30 Hz ("beta-band" activity) over a period from 500-1000 Hz. These frequency bands were chosen a priori based on commonly reported values in the literature (e.g., 24-25), and this specific temporal window was chosen a priori based on prior reports suggesting that it takes human observers ~300-500 ms to process and respond to a retrospective memory cue (e.g., 60).

To visualize changes in occipitoparietal alpha power, frontocentral mu-alpha power, and frontocentral beta power, we extracted and averaged lateralization estimates from 8-13 Hz over electrode sites O1/2, PO3/4, and PO7/8, lateralization estimates from 8-13 Hz over electrode sites C1/2, C3/4, and lateralization estimates from 15-30 Hz over electrode sites C1/2, C3/4. Statistical analyses of lateralization were

performed using nonparametric sign permutation tests with temporal cluster-based correction (see *Statistical Analyses*, below).

Quantifying Eye Position Biases. Preprocessed eye position data were sorted by the location of the retrospectively cued stimulus (i.e., left vs. right visual field). Since stimuli were rendered along the vertical meridian, we restricted our analyses to horizontal eye position measurements. Following earlier work (28), we computed a normalized measure of gaze bias by converting pixelwise recordings into a percentage along an axis extending from fixation to the center of each visual stimulus. Thus, a ±100% gaze bias would result from participants foveating the center of one stimulus, while a 0% gaze bias would result from participants perfectly holding fixation. Gaze biases during right visual field trials were sign reversed and averaged with biases from left visual field trials, yielding a single gaze position bias time course per participant.

Decoding Stimulus Orientation. Orientation decoding analyses were performed on broadband (1-50 Hz) signals measured at occipitopartietal electrode sites O1/2, PO3/4, PO7/8 and frontocentral electrode sites C1/2, C3/4. Decoding performance was computed separately for each time sample using 10-fold cross-validation. During each cross-validation fold, we designated 90% of available trials as a training data set and the remaining 10% of trials as a test data set, taking care to ensure that the training data set contained an equal number of observations for each possible outcome. Decoding performance was estimated using the multivariate distance between EEG activity patterns associated with memory for specific experimental conditions (61). We computed the Mahalanobis distance between trial-wise activation patterns in each test data set with position-specific activation patterns in the corresponding test data set,

yielding a location-wise set of distance estimates. If scalp activation patterns contain information about stimulus orientation, then distance estimates should be smallest when comparing patterns associated with memory for similar or identical conditions in the training and test data sets and largest when comparing opposite conditions. Trial-wise distance functions were averaged and sign-reversed for interpretability. Decoding performance was estimated by convolving timepoint-wise distance functions with a cosine function, yielding a metric where chance decoding performance is equal to 0. Decoding results from each training- and test-data set pair were averaged (thus ensuring the internal reliability of our approach), yielding a single decoding estimate per participant, timepoint, and task condition. To facilitate interpretability, orientation decoding timeseries were smoothed with a 50 ms Gaussian kernel. We verified that smoothing did not qualitatively affect any of the findings reported in the manuscript.

In supplementary analyses, we also attempted to decode stimulus orientation from a broader set of 32 occipitoparietal electrodes, or from all 62 scalp electrodes. These analyses yielded results quantitatively identical to those shown in Figure 3A.

Statistical Comparisons - General. Statistical comparisons were based on nonparametric signed randomization tests (62). Unless otherwise specified, each test we performed assumes a null statistic of 0 (i.e., no difference in alpha- or beta-band lateralization, or no difference in observed vs. chance decoding performance). We therefore generated null distributions by randomly relabeling each participant's data with 50% probability and averaging the data across participants. This step was repeated 10,000 times, yielding a 10,000-element null distribution for each time point. Finally, we implemented a cluster-based permutation test with cluster-forming and cluster-size

thresholds of $p < 0.05$ (two-tailed) to evaluate observed differences with respect to the null distribution while correcting for signal autocorrelation.

Statistical Comparisons – Latency Differences. To compare the latencies of various signals (e.g., lateralized alpha-band EEG activity and gaze biases; Fig 2) we implemented a bootstrapping routine. In the first step of the analysis, we randomly selected, with replacement, and averaged data from N of N experimental participants (where N is the total number of participants available for a given analysis, i.e., 31 for comparisons of EEG signals and 18 for comparisons of gaze bias and EEG signals), yielding a single time-series per measurement. Next, we estimated the onset (or offset) of significant (i.e., non-zero) activity using the cluster-based permutation test approach described in the preceding section, yielding a single latency estimate per signal. These two steps were repeated 10,000 times, yielding 10,000 element distributions of latency estimates for each signal. Finally, we computed the number of times where latencies for one signal were greater than (or less than, depending on the contrast) the other signal. Dividing this number by the total number of permutations yields an empirical p-value.

References

1. D'Esposito M, Postle BR. The cognitive neuroscience of working memory. Annual Review of Psychology, 66:115-142 (2015)

2. Buschman TJ. Balancing flexibility and interference in working memory. Annual Review of Vision Science, 7:367-388 (2021)

3. van Ede F., Nobre AC. Turning attention inside out: How working memory serves behavior. Annual Review of Psychology (2022)

4. Heuer A, Ohl S, Rolfs M. Memory for action: A functional view of selection in working memory. Visual Cognition 28 (2020)

5. Olivers CNL, Roelfsema PR. Attention for action in visual working memory. Cortex 131:179-194 (2020)

6. Gonzalez-Garcia C, Formica S, Liefooghe B, Brass M. Attentional prioritization reconfigures novel instructions into action-oriented task sets. Cognition 194:104059 (2020)

7. Ohl S, Rolfs M. Bold moves: Inevitable saccadic selection in visual short-term memory. Journal of Vision 20(2):11 (2020)

8. Tang C, Herikstad R, Parthasarathy A, Libedinsky C, Yen S-C. Minimally dependent activity subspaces for working memory and motor preparation in the lateral prefrontal cortex. eLife:9e58154 (2020)

9. Pho GN, Goard MJ, Woodson J, Crawford B, Sur M. Task-dependent representations of stimulus and choice in mouse parietal cortex. Nature Communications, 9:1-16 (2018)

10. Panichello M, Buschman T. Shared mechanisms underlie the control of working memory and attention. Nature 592:601-605 (2021)

11. Chatham CH, Frank MJ, Badre D. Corticostriatal output gating during selection from working memory. Neuron 81:930-942 (2014)

12. Minxha J, Adolphs R, Fusi S, Mamelak AN, Rutishauser U. Flexible recruitment of memory-based choice-representations by the human medial frontal cortex. Science, 368:eaba3313 (2020)

13. Galero-Salas Y, Han S, Sych Y, Voigt FF, Laurenczy B, Gilad A, Helmchen F. Sensory and behavioral components of neocortical signal flow in discrimination tasks with short-term memory. Neuron, 109:135-148 (2021)

14. Rac-Lubashevsky R, Frank MJ. Analogous computations in working memory input, output and motor gating: Electrophysiological and computational modeling evidence. PLoS Computational Biology 17:e1008971 (2021)

15. Henderson MM, Rademaker RL, Serences JT. Flexible utilization of spatial- and motor-based codes for the storage of visuo-spatial information. eLife, 11:e75688 (2022)

16. Ariani G, Pruszynski JA, Diedrichsen J (2022) Motor planning brings human primary somatosensory cortex into action-specific prepatory states. eLife 11:e69517 (2022)

17. van Ede F, Chekroud SR, Stokes M, Nobre AC. Concurrent visual and motor selection during visual working memory guided behavior. Nature Neuroscience, 22:477-483 (2019)

18. van Ede F, Deden J, Nobre AC. Looking ahead in working memory to guide sequential behavior. Current Biology 31:R779-R780 (2021)

19. Naswari R, van Ede F. Planning the potential future during multi-item visual working memory. Journal of Cognitive Neuroscience 34:1534-1546 (2021)

20. Boettcher SEP, Gresch D, Nobre AC, van Ede F. Output planning at the input stage in visual working memory. Science Advances 7:eabe8212 (2021)

21. Cisek P. Resynthesizing behavior through phylogenetic refinement. Attention, Perception & Psychophysics, 81:2265-2287 (2019)

22. Cisek P, Kalaska JF. Neural mechanisms for interacting with a world full of action choices. Annual Review of Neuroscience 33:269-298 (2010)

23. van Ede F. Mnemonic and attentional roles for states of attenuated alpha oscillations in perceptual working memory: a review. European Journal of Neuroscience, 48:2509-2515 (2018)

24. Klimesch W. Alpha-band oscillations, attention, and controlled access to stored information. Trends in Cognitive Sciences, 16:606-617 (2012)

25. Jenkinson N, Brown P. New insights into the relationship between dopamine, beta oscillations, and motor function. Trends in Neurosciences, 34:611-618 (2018).

26. Libby A, Buschman TJ. Rotational dynamics reduce interference between sensory and memory representations. Nature Neuroscience 24:715-726 (2021)

27. Wan Q, Menendez JA, Postle BR. Priority-based transformations of stimulus representation in visual working memory. PLOS Computational Biology 18:e1009062 (2022)

28. van Ede, F., Chekroud, S.R., & Nobre, A.C. Human gaze tracks attentional focusing in memorized visual face. Nature Human Behavior 3:462-470. (2019).

29. van Ede F., Board AG, Nobre AC. Goal-directed and stimulus-driven selection of internal representations. Proceedings of the National Academy of Sciences, 17:24590-24598

30. van Ede F, Deden J, Nobre AC. Looking ahead in working memory to guide sequential behavior. Current Biology 31:R779-R780 (2021)

31. Thom, J.L., Nobre, A.C., van Ede, F,. & Drashckow, D. (2022). Head direction tracks internally directed selective attention in visual working memory. bioRxiv

32. Liu, B., Nobre, A.C., & van Ede, F. Functional but not obligatory link between microsaccades and neural modulation by covert spatial attention. Nature Communications, 13*:*3503. (2022).

33. Yu G, Herman JP, Katz LN, Krauzlis RJ. Microsaccades as a marker not a cause for attention-related modulation. eLife 11:e74168 (2022)

34. Foster JJ, Bsales EM, Jaffe RJ, Awh E. Alpha-band activity reveals spontaneous representations of spatial position in visual working memory. Current Biology, 27:3216-3223 (2017)

35. Golomb, J.D., L'Heureux, Z.E., & Kanwisher, N. (2014). Feature-binding errors after eye movements and shifts of attention. *Psychological Science, 25*(5), 1067-1078.

36. Golomb, J.D., Kupitz, C,N., & Thiemann, C.T. (2014). The influence of object location on identity: A spatial congruency bias. *Journal of Experimental Psychology: General, 143*(6), 2262-2278.

37. Dill, M., & Fahle, M. (1998). Limited translation invariance of human visual pattern recognition. *Perception & Psychophysics, 60*(1), 65–81.

38. Zaksas, D., Bisley, J. W., & Pasternak, T. (2001). Motion information is spatially localized in a visual working-memory task. *Journal of neurophysiology*, *86*(2), 912–921.

39. Hollingworth, A. (2007). Object-position binding in visual memory for natural scenes and object arrays. *Journal of Experimental Psychology: Human Perception and Performance, 33*(1), 31–47.

40. Groen, I.I.A., Dekker, T.M., Knapen, T., & Silson, E.H. (2022). Visuospatial coding as ubiquitous scaffolding for human cognition. *Trends in Cognitive Sciences, 26*(1), 81-96.

41. Wolff MJ, Jochim J, Akyurek EG, Stokes MG. Dynamic hidden states underlying working-memory-guided behavior. Nature Neuroscience 20:864-871 (2017)

42. Rose, N. S., LaRocque, J. J., Riggall, A. C., Gosseries, O., Starrett, M. J., Meyering, E. E., & Postle, B. R. (2016). Reactivation of latent working memories with transcranial magnetic stimulation. *Science (New York, N.Y.)*, *354*(6316), 1136–1139.

43. Sprague TC, Ester EF, Serences JT. Restoring latent visual working memory representations in human cortex. Neuron 91:694-707 (2016)

44. Ester EF, Nouri A, Rodriguez L. Retrospective cues mitigate information loss in human cortex during working memory storage. Journal of Neuroscience, 38:8538-8548 (2018)

45. Barbosa, J., Lozano-Soldevilla, D., & Compte, A. (2021). Pinging the brain with visual impulses reveals electrically active, not activity-silent, working memories. *PLOS Biology, 20*(3), e3001603.

46. Bae, G.Y., & Luck, S.J. (2018). Dissociable decoding of spatial attention and working memory from EEG oscillations and sustained potentials. *Journal of Neuroscience 38*(2), 409-422.

47. Serences JT, Ester EF, Vogel EK, Awh E. Stimulus-specific delay activity in human primary visual cortex. Psychological Science 20:207-214 (2009)

48. Ester EF, Anderson DE, Serences JT, Awh E. A neural measure of precision in visual working memory. Journal of Cognitive Neuroscience 25:754-761.

49. Ester EF, Rademaker RL, Sprague TC. How do visual and parietal cortex contribute to visual short-term memory? eNeuro 3 (2016)

50. Zhao Y-J, Kay KN, Tian Y, Ku Y. Sensory recruitment revisited: Ipsilateral V1 involved in visual working memory. Cerebral Cortex 32:1470-1479 (2022)

51. Scimeca JM, Kiyonaga A, D'Esposito M. Reaffirming the sensory recruitment account of working memory. Trends in Cognitive Sciences 22:190-192 (2018)

52. van Ede F. Visual working memory and action: functional links and bi-directional influences. Visual Cognition 28:401-413 (2020)

53. Nobre AC, Stokes MG. Preremembering experience: A hieractchy of time-scales for proactive attention. Neuron 104:132-146 (2019)

54. Luck SJ. An introduction to the event-related potential technique, 2nd Edition. MIT Press, 2014

55. Kleiner M, Brainard D, Pelli D. What's new in Psychtoolbox-3? iPerception 36 (2007)

56. Delorme A, Makeig S. EEGLAB: An open-source toolbox for analysis of single-trial EEG dynamics including independent component analysis. Journal of Neuroscience Methods 134:9-21 (2004)

57. Chang C-Y, Hsu S-H, Pion-Tonachini L, Jung T-P. Evaluation of Artifact Subspace Reconstruction for automatic artifact components removal in multi-channel EEG recordings. IEEE Transactions on Biomedical Engineering, 67(4) (2019)

58. Blum S, Jacobsen NSJ, Bleichner MG, Debener S. A Reimannian modification of Artifact Subspace Reconstruction for EEG artifact handling. Frontiers in Human Neuroscience 141 (2019)

59. Perrin F, Pernier J, Bertrand O, Echallier JF. Spherical splines for scalp potential and current density mapping. Electroencephalography and Clinical Neurophysiology, 72:184-187 (1989)

60. Souza, A.S., Rerko, L., & Oberauer, K. (2014). Unloading and reloading working memory: Attending to one item frees capacity. *Journal of Experimental Psychology: Human Perception & Performance 40*(3), 1237-1256.

61. Wolff MJ, Kandemir G, Stokes MG, Akyurek EG. Unimodal and bimodal access to sensory working memories by auditory and visual impulses. Journal of Neuroscience, 40:671-681 (2020)

62. Maris E, Oostenveld R. Nonparametric statistical testing of EEG and MEG data. Journal of Neuroscience Methods, 164:177-190 (2007)

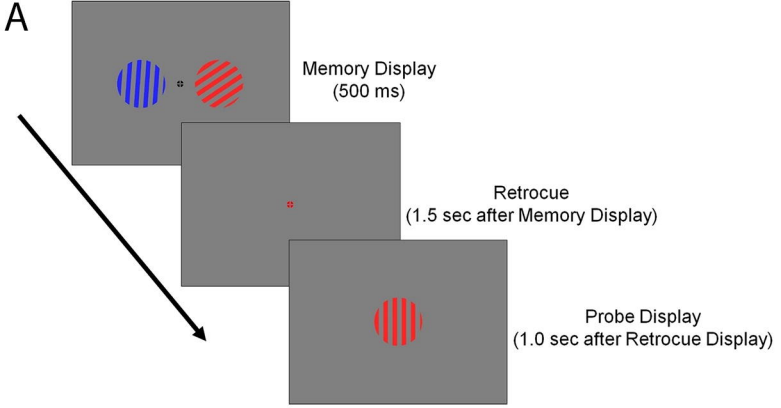
A
Memory Display
(500 ms)
Retrocue
(1.5 sec after Memory Display)
Probe Display
(1.0 sec after Retrocue Display)

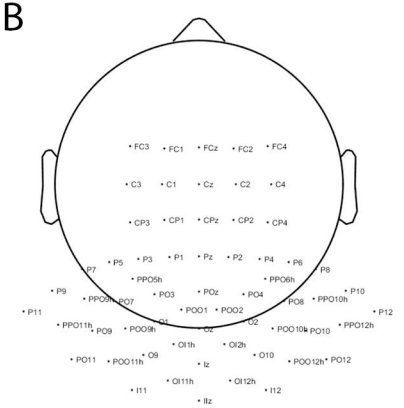
B
FC3
FC1
FCz
FC2
FC4
C3
C1
Cz
C2
C4
CP3
CP1
CPz
CP2
CP4
P7
P5
P3
P1
Pz
P2
P4
P6
P8
PPO5h
PPO6h
P9
PPO9h
PO7
PO3
POz
PO4
PO8
PPO10h
P10
P11
POO1
POO2
P12
PPO11h
PO9
POO9h
O1
Oz
O2
POO10h
PO10
PPO12h
OI1h
OI2h
O9
O10
PO11
POO11h
Iz
POO12h
PO12
OI11h
OI12h
I11
I12
IIz

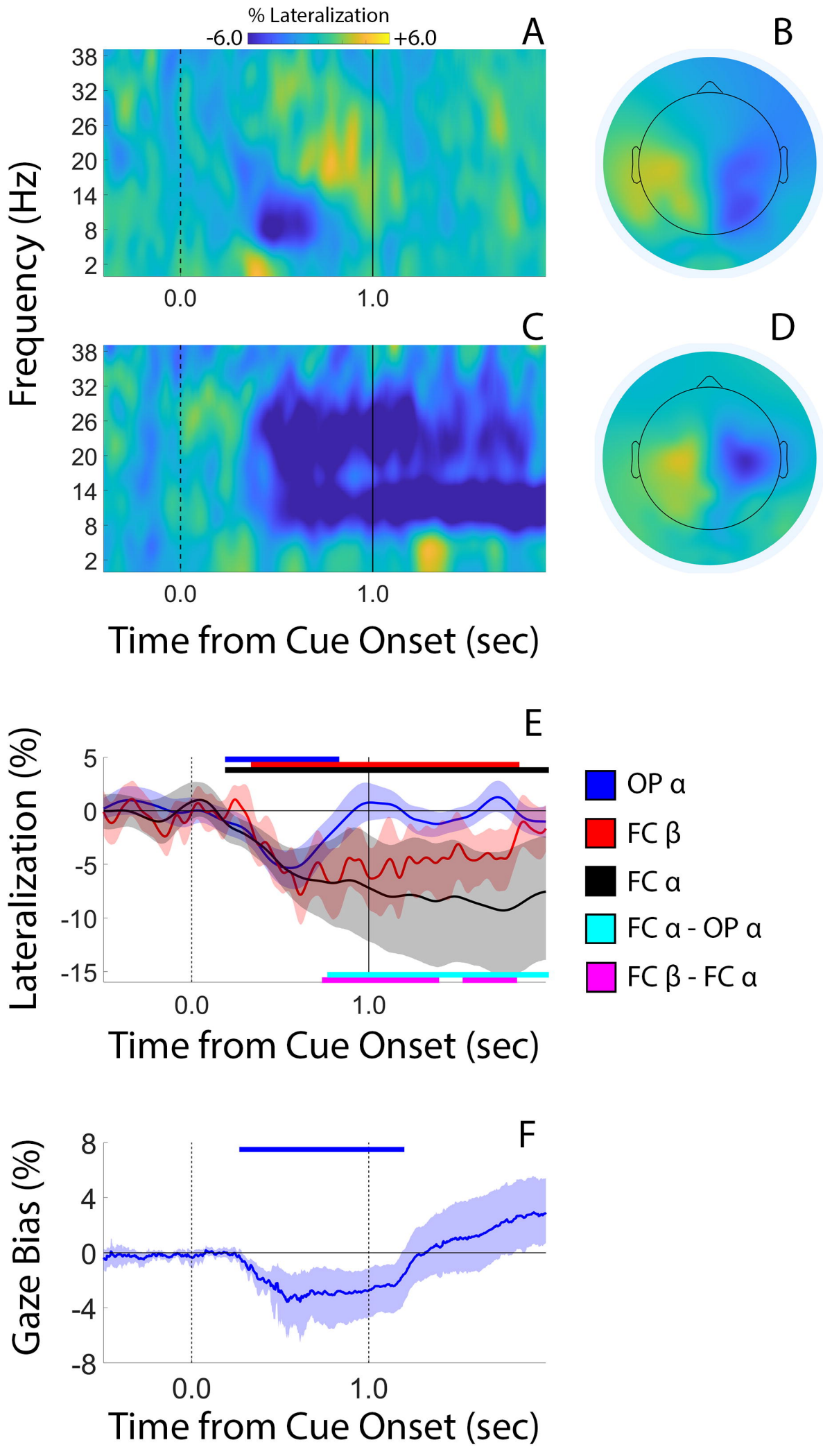
% Lateralization
-6.0
+6.0
A
B
C
D
E
F
Frequency (Hz)
38
32
26
20
14
8
2
0.0
1.0
Time from Cue Onset (sec)
Lateralization (%)
5
0
-5
-10
-15
OP α
FC β
FC α
FC α - OP α
FC β - FC α
Gaze Bias (%)
8
4
0
-4
-8

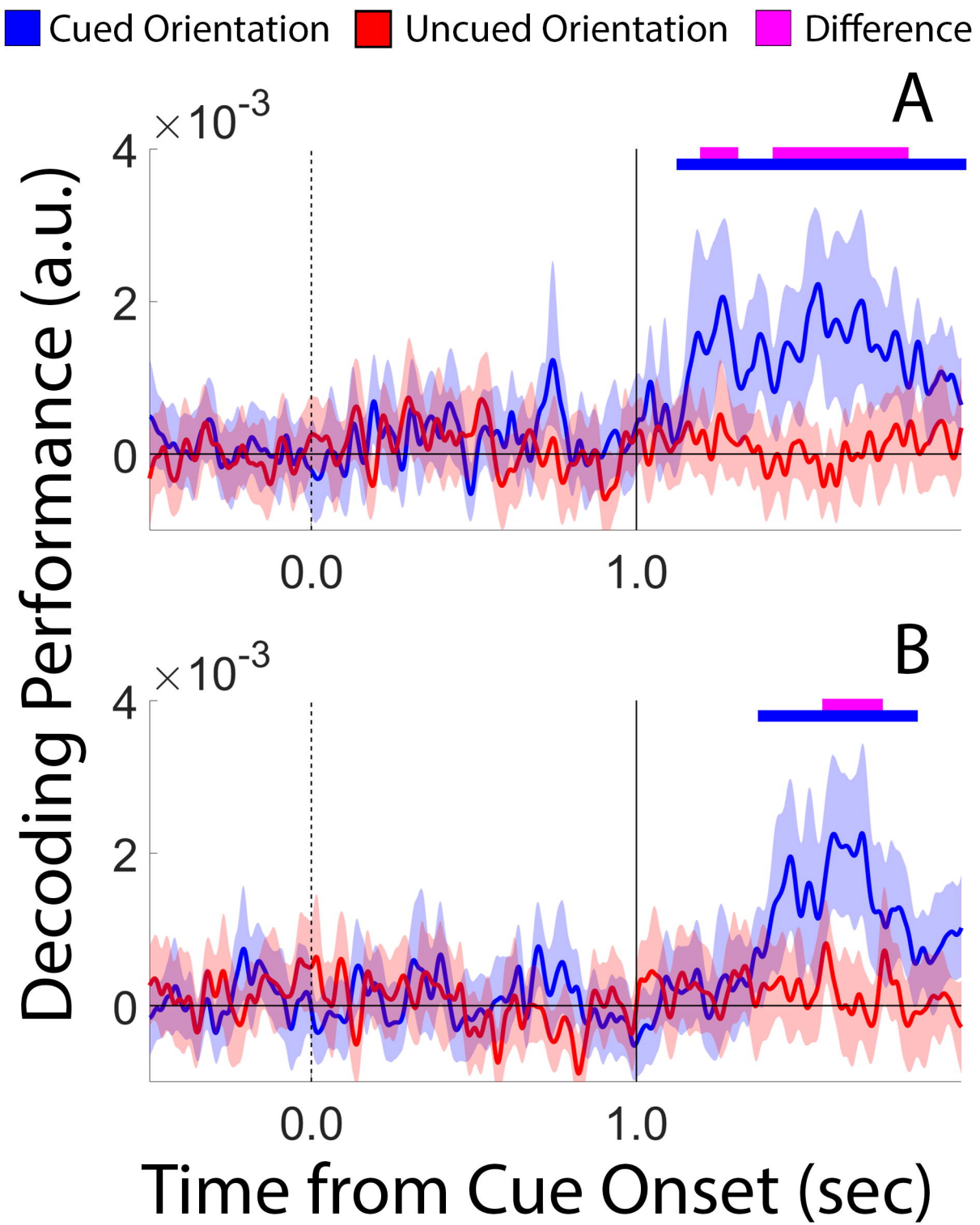
Cued Orientation
Uncued Orientation
Difference
A
B
×10-3
4
2
0
0.0
1.0
Decoding Performance (a.u.)
Time from Cue Onset (sec)